Int J Adv Manuf Technol (2015) 80:343–360
DOI 10.1007/s00170-015-7004-7

ORIGINAL ARTICLE

An experimental investigation of surface modification of C-40 steel using W–Cu powder metallurgy sintered compact tools in EDM

P. K. Patowari[1] · P. Saha[2] · P. K. Mishra[3]

Received: 3 February 2012 / Accepted: 9 March 2015 / Published online: 24 March 2015

Abstract Surface modification is essential to enhance the surface properties of engineering components. This may be accomplished either in the form of altering the surface chemistry or by providing a protective layer over the work surface. In this paper, the surface modification phenomenon by depositing a protective layer over the work surface by electrical discharge machining (EDM) is presented. The potential of EDM, which is otherwise a useful non-conventional machining process, has been explored for surface alteration by depositing material over work surface using tungsten–copper (W–Cu) sintered powder metallurgy tools. The photographic presentation of the EDMed surface at different parameter settings is given. The variations of mass transfer rate (MTR), deposited layer thickness (LT), and average surface roughness (R_a) with various parameter combinations are presented in graphical form and their effects are discussed. A wide spectrum of MTR ranging from nearly 1 to 191 mg/min and average surface roughness values ranging from 3 to 15 μm have been achieved. A wide range of deposited layers with thickness varying from 3 to 785 μm has been achieved by various combinations of process parameters. The microstructure of the deposited layers with microhardness at different zones is presented. It has been observed that the microhardness is gradually increasing from the base material to the deposited layer and its maximum value is found to be 15.7 GPa at the hardest zone. SEM, EDX, and XRD analyses has been also performed for further characterization of the deposited layer. A quantitative analysis of the layer has been carried out by EDX and it is found that the inner part of the layer is richer in tungsten than the superficial surface. This contributed towards the higher hardness of the layer at the core.

Keywords Electrical discharge machining · EDM · Surface modification · P/M compact tool · Mass transfer rate · Layer deposition

P. K. Patowari is associate professor, National Institute of Technology Silchar, and holds a PhD.
P. Saha is associate professor, Indian Institute of Technology Kharagpur, and holds a PhD.
P. K. Mishra is professor emeritus, Indian Institute of Technology Bhubaneswar, and holds a PhD.

✉ P. K. Patowari
ppatowari@yahoo.com

P. Saha
psaha@mech.iitkgp.ernet.in

P. K. Mishra
pkm@iitbbs.ac.in

[1] Department of Mechanical Engineering, National Institute of Technology, Silchar 788010, Assam, India

[2] Department of Mechanical Engineering, Indian Institute of Technology, Kharagpur 721302, West Bengal, India

[3] Department of Mechanical Engineering, Indian Institute of Technology, Bhubaneswar 751013, India

1 Introduction

In engineering applications, a material is often selected to satisfy the strength requirement of the parts, but the selected material may not possess satisfactory surface properties. Engineering components when subjected to aggressive environments like high speed, corrosive media, extreme temperatures, and cyclic stresses result in failure initiated due to surface degradation. An advanced material having excellent friction, wear, corrosion, and fatigue properties is much desirable in frontier technology applications in aerospace, power generat ion, nuclear, and automobile industries. In addition, it is also essential to use a suitable protective coating over the exposed surface to minimize wear erosion, high-temperature oxidation,

and corrosion. Surface modification methods are normally dedicated processes for surface treatment or surface coating only. Now, the question arises whether it is possible to incorporate the surface modification phenomenon within the manufacturing process itself. Can some secondary effect of a manufacturing process on a workpiece surface during processing be turned into a useful surface modification method? If it is possible, then the workpiece surface can be tailored during the manufacturing process itself in the same setting of parts fabrication and it becomes an added advantage to the process. A thought in this direction leads towards the idea of considering electrical discharge machining (EDM) as a potential manufacturing process where some alteration of material takes place on the surface during processing. This alteration is in the form of white layer or recast layer, which otherwise, is a disadvantage to the process. So, this disadvantage can be turned into a useful surface treatment technique by proper control of operating parameters and tool material. Thus, the formation of white layer is the main source of inspiration for the researchers to study the surface modification phenomena in EDM.

It has been reported that EDMed surface contains a hard and cracked recast layer and heat affected zone underneath [1]. The topmost layer is a recast layer formed by resolidification of the molten metal at the base of the craters after the discharge [2]. This layer is found to be heavily alloyed with the products of pyrolysis of the cracked dielectric. Rebelo et al. [3] attempted a semi-quantitative analysis of the carbon content in the surface layers. The carbon content was found to be up to nine times higher at the surface than that in the bulk material. It was reported by Cusanelli et al. [4] that the white layer is a result of solidification of the melted zone and it exhibits high hardness, good adherence to the bulk and good resistance to corrosion. However it contains microcracks, which may constitute a problem for certain applications. For deliberate change in surface properties, several techniques such as EDM with powder metallurgy (P/M) compact tool, EDM with thin wires, and EDM with powder suspended in working oil have been attempted by many researchers.

Many studies have been reported using this technique of surface modification by EDM with P/M tools. In these studies, the P/M tool is considered as the main source of material for coating on to the workpiece. So the tool needs to erode significantly in this type of treatment. There was an attempt by Gangadhar et al. [5] to transfer bronze on to steel work surface by electrical discharge processing. It was found that the anodic material transfer to the cathode was very significant. Shunmugam et al. [6] further reported that using a hard and wear-resistant material in the compact, the wear resistance of the resultant surface could be improved. The performance of P/M electrodes on various aspects of EDM operation was also discussed by Samuel et al. [7]. Surface modification by EDM using composite structured tool consisting of green compact products or sintered products was reported by Mohri et al. [8]. There were further reports in this area by several researchers like Fukuzawa et al. [9, 10], Mohri et al. [11], and Moro et al. [12]. Surface modification of aluminum and aluminum matrix composite with a tool of Ti-36mass%Al premixed green compact was carried out by Tsunekawa et al. [13, 14]. The feasibility of surface hardening and alloying of tool steels using sintered 70Fe-30WC tools leading to the formation of a surface alloyed layer consisting of anti-wear constituents like carbides was studied by Pantelis et al. [15]. Simao et al. [16, 17], Aspinwall et al., [18], and Lee et al. [19] published different studies on electrical discharge texturing (EDT) using P/M tools made from TiC/WC/Co and WC/Co powders. Wang et al. [20] discussed the method of electrical discharge coating (EDC) by using a titanium powder green compact tool. Use of copper and chromium powder-blended tools was proposed by Tsai et al. [21] to facilitate the formation of a modified surface layer on the workpiece after EDM, with remarkable corrosion resistant properties. Akiyoshi et al. [22] reported the use of metallic material that makes hard carbides such as titanium and wolfram (tungsten) as tool material in electrical discharge coating (EDC). Yan et al. [23] investigated the feasibility of modifying the surface of pure titanium metal by adding urea into the dielectric that resulted in TiN ceramic layer over the workpiece. The significant alteration of the elemental composition of dental alloy surfaces after EDM treatment was reported by Zinelis [24]. Chen et al. [25] investigated how machining characteristics and surface modifications affect low-carbon steel during EDM processes with semi-sintered electrodes. They confirmed that the composition of the semi-sintered electrodes can be transferred onto the machined surface efficiently and effectively during the EDM process and the process can easily form a modified layer on the machined surface.

An endeavor towards experimental investigation of the process using WC-Cu and W–Cu P/M electrodes was made by the authors [26, 27]. Taguchi technique of DOE was adopted to conduct the first set of experiments to identify the influential parameters and optimal conditions were achieved for a uniformly deposited layer. A detailed experimental study towards the surface integrity of C-40 steel processed with WC-Cu P/M green compact tools in EDM was also reported by the authors [28].

In the present paper, authors are reporting the detailed studies, especially on the aspect of material transfer and deposited layer, in surface modification phenomenon using W–Cu P/M tools in EDM. Attempt has been made to deposit hard layer of carbides of tungsten over the work surface. For this purpose, tungsten with copper (W75%–Cu25% by weight) is chosen as the material of P/M compact tools. The effect of different controlling parameters like composition, compaction pressure, sintering temperature, pulse on time, pulse off time,

and peak current setting are reported. Further, a qualitative as well as a quantitative analysis of the deposited layer is also presented which has been carried out using SEM, XRD, and EDX analyses.

2 Experimentation

2.1 Equipments, electrode, and workpiece

Electric discharge machining was carried out on a die sinking EDM (model: Victor-I, manufacturer: Electronica Machine Tool Ltd., India). Rustlick™ EDM oil of grade EDM 30 has been used as dielectric fluid. Tungsten and copper powders of mesh -325 were used as tool material. These powders of required composition (W75%–Cu25% by weight) were mixed and compacted at different pressures and then sintered at definite temperature in hydrogen atmosphere in a tubular furnace for 1 h. The powder metallurgy (P/M) tools, having loose bonding of powder particles, exhibits appreciable amount of tool material transfer over the work surface. Semi-sintered tools were used because the sintering process provides some strength to the P/M compacts, hence the tools can easily be handled and at the same time these can serve the purpose of tool material transfer to the workpiece. The powder particles eroded from the tool react with the carbon particles, which are liberated due to the breakdown of dielectric medium, i.e., the hydrocarbon oil, and form the carbides. The hard carbides deposited on the work surface result in hard layer on the work surface. The dimension of cylindrical compacts was 12.5 mm in diameter and 6 to 8 mm in height. These compacts were then glued to copper holders using an electrically conductive paste. The workpiece was made of C-40 grade steel, and of dimensions 16 mm×16 mm×5 mm. The constituents of the workpiece material, found by chemical analysis, were as follows: 0.45–0.46 % C, 0.34 % Mn, 0.24 % Si, 0.028 % S, 0.031 % P, and rest iron.

2.2 Experimental procedure

Experiments were conducted at various combinations of investigating parameters. In this paper, their effects on material transfer rate (MTR), average layer thickness (LT), and surface roughness (R_a) are presented. MTR was measured by taking mass difference of the workpiece and tool before and after EDM, using a precision electronic balance (model: Afcoset, ER-182). Surface roughness of the EDMed surface was measured using a surface profilometer (make: Taylor Hobson, model: Surtronic 3+). To find out the deposited layer thickness, each workpiece was sectioned in the transverse direction using WEDM and then mounted properly keeping the sectioned area exposed. Mounting prevents the rounding of the edges during polishing of the specimen. The mounted specimen was then polished and etched with 2 % Nital solution for 20 s in order to reveal the deposited layer over the substrate. The layer thickness was measured along the entire length of deposited portion at a regular interval of 200 μm and the average value was calculated. Microhardness was measured at different zones in transverse section of work surface after proper polishing with a microhardness tester (Leco M-400-H1). The micrographs of deposited layer were captured by an optical microscope (Leica DMRX). To ascertain the phases present in the deposited layer, XRD was done on the EDMed samples using Philips X-ray diffractometer and the analysis was done using PCPDF data files and Philips X'pert High Score software. Scanning electron micrographs (SEM) of the EDMed surface were taken using the JEOL-JSM 5800 scanning electron microscope. EDX was also done in the same SEM setup.

2.3 Experimental parameters

To conduct this study, the experimental parameters were selected as given in Table 1. All the experiments were conducted in an electrode (–) polarity setting, because this gives higher tool wear. Gap control was so adjusted that the average gap voltage was maintained at around 40–45 V. The EDMing time was kept constant for 5 min, so that the significant effect can be observed in the entire range of the experiments.

3 Experimental results

3.1 Photographic representation of EDMed samples

The photographs of some specimens after EDM operation give the first impression of the outcome. Samples at different parameter settings are shown in Fig. 1. A very fine and uniform coating can be observed at lower T_{on} settings with lower Ip settings with tools sintered at 700 °C. But with the increase in T_{on} and T_{off} and Ip setting, the surface becomes extremely

Table 1 Experimental parameters

Parameters	Description
Electrode composition	75 % tugnsten–25 % copper by weight
Compaction pressure (CP)	120, 180, 240, and 300 MPa
Sintering temperature (ST)	700 and 900 °C
Peak current setting (Ip)	4, 8, 10, and 12 A
Pulse duration (T_{on})	Minimum19 μs to maximum 386 μs
Polarity	Electrode (−)
Duty factor (DF)	At lower T_{on} settings, 50 % and At higher T_{on} setting, at 70 %.
Gap voltage	40–45 V
Processing time:	5 min

Fig. 1 Representative photographs of workpieces processed at different parameter settings as mentioned

uneven. This can be observed in Fig. 1b. The tool of low compaction pressure (120 MPa) cannot withstand the shock generated due to the discharge at 12 A and results in small fragmented particles, which in turn produces severe arcing. The black spots on the deposited surface are due to the occurrence of arcing on these spots.

The tools made with sintering temperature of 700 °C result in more mass transfer than that by the tool sintered at 900 °C at lower current settings like 4–8 A. On the other hand, tools sintered at 900 °C can withstand higher current. Tools with low compaction pressure at lower T_{on} settings and higher Ip settings results in some mass transfer as shown in Fig. 1c. But the tools with higher compaction pressure like 300 MPa do not help much in mass transfer even at higher T_{on} settings. Neither there was any indication of surface damage nor there was much mass transfer taking place as evident from in Fig. 1d. So, at pressure 120 MPa, some material deposition can be observed but with the increase of compaction pressure this reduces and at 300 MPa material removal rather than deposition takes place.

Some experimental results with tools sintered at 700 °C at different parameter settings like T_{on} 256 μs and 386 μs; Ip 4, 6, 8, and 10 A are shown in Figs. 2 and 3. The effects of Ip and compaction pressure at higher T_{on} can be observed clearly in Fig. 2. At 4 A, the amount of mass transfer is less and the surface is not so uniform. Whereas, Ip setting of 8 A is giving good result in this respect. Further, workpieces processed at different Ip settings and at T_{on} of 256 μs are shown in Fig. 3. It can be observed that with the increase of Ip, the mass transfer increases. It is also found that at T_{on} 126 μs, and at lower current settings like 4 and 6 A, mass transfer is less and work surface is rough. But at 8 and 10 A, surface becomes smooth. This can be attributed to the fact that at lower current, the energy supplied to the process is not sufficient to sustain constant mass transfer all over due to the interruptions in mass flow and thus gives rise to an irregular surface finish.

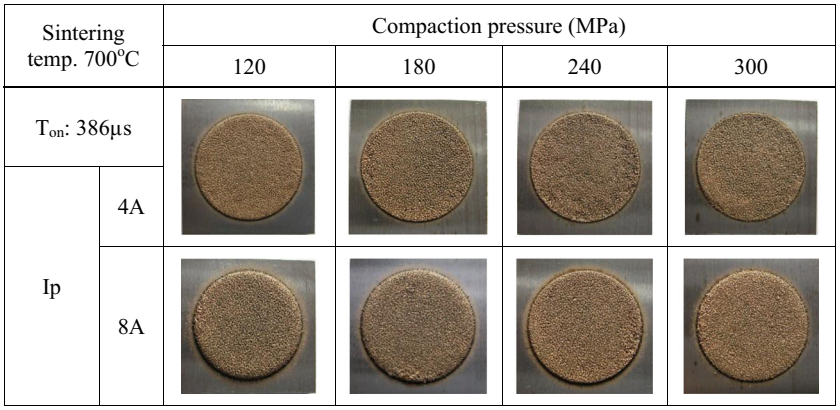

Fig. 2 Workpieces processed with tools at different compaction pressure and ST 700 °C and at Ip 4 and 8 A, T_{on} 386 μs

When the current is increased to 8 and 10A, the free flow of mass occurs resulting in a regular surface. But it is already observed that the increase of current beyond certain limit is also not helpful. The tool should not be subjected to gradual disintegration at that high current. On the other hand, as shown in Fig. 3, at T_{on} 256 μs and Ip of 6A onwards, the surface is rather uniform. Here, the duration of supplying the energy per pulse is more that helps in uniform mass transfer. At T_{on} of 386 μs and at 4 A, the deposited surface is very smooth. Neither a very low current setting nor a very high current setting is acceptable to the process. In combination with current setting, an appropriate selection of pulse duration is also necessary.

3.2 Material transfer rate

The reported Material Transfer Rate (MTR) is the net MTR on the work surface. A simple method has been followed to measure the MTR. The mass of the workpiece was recorded with a precision electronic balance before and after the EDM operation for a specific time. The difference of the mass divided by the time gives the MTR. If the deposition is taking place, then there will be gain in mass and hence positive MTR and if the machining is taking place then there will be reduction in mass and hence negative MTR. The phenomena of material removal and material transfer occur simultaneously during processing in EDM. The tool material is getting transferred from the tool to the molten pool of the workpiece material during discharge and at the same time some portion of the material are flushed out also from this zone. As a result the amount which is retained on the work surface is the net material transfer. Hence, MTR was measured by taking the mass difference of the workpiece before and after EDM for a particular time period. The positive values indicate material addition rate and the negative values indicate material removal rate. The variation of MTR with different parameters is shown in Figs. 4, 5, 6, and 7, and from these plots following inference can be made.

- In the plots of MTR-T_{on} with the tools sintered at 700 °C at different compaction pressure as shown in Fig. 4a, b, c, it can be observed that for all Ip and T_{on}, settings there is addition of materials. With the increase in T_{on}, the MTR increases. At lower compaction pressure, the MTR is more than that at higher compaction pressure. It can be noted from these plots that with the increase in compaction pressure MTR decreases. At higher T_{on} settings, this trend is more prevalent.
- With the tools sintered at 900 °C, it is seen that at lower compaction pressure, i.e., 120 MPa, there is net addition of mass. But with the tools of higher compaction pressure material removal is observed rather than addition. These things can be clearly observed with the plots of MTR-T_{on} at ST 900 °C in Fig. 5a, b. With the increase in T_{on}, MTR as well as MRR (negative MTR) are increasing as is the situation.
- In a few experiments conducted with the tools of compaction pressure 120 MPa, sintering temperature 700 °C and T_{on} settings 126 and 256 μs, it is observed that with the increase in Ip, the MTR increases. This is shown in the

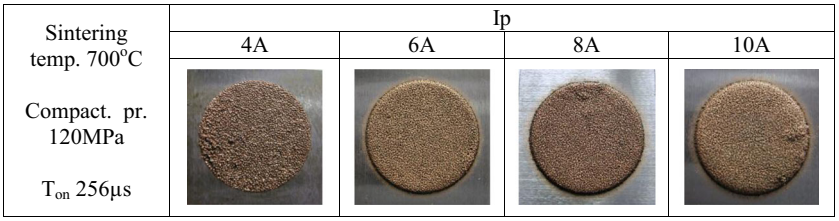

Fig. 3 Workpieces processed at different Ip at T_{on} 256 μs, with tools compaction pressure 120 MPa and sintering temperature 700 °C

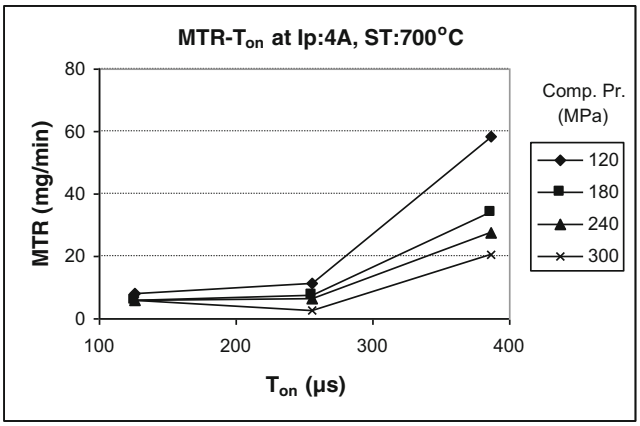

(a)

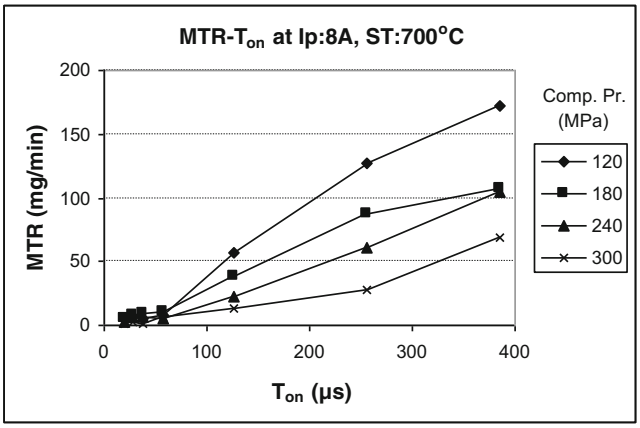

(b)

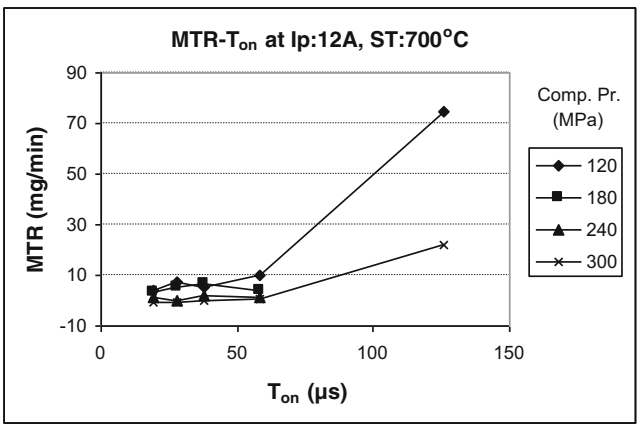

(c)

Fig. 4 The variation of MTR with T_{on} at different compaction pressures, at ST 700 °C and **a** Ip 4 A, **b** Ip 8 A, **c** Ip 12 A

plot of MTR-Ip in Fig. 6. In this plot, it can be seen that at T_{on} 256 µs, MTR is more than that at 126 µs. In the curve of T_{on} 256 µs, it is seen that at 12 A, MTR decreases. This is because of occurrence of arcing at this higher Ip and T_{on} settings which prevents the process to occur smoothly.

- The plots showing the variations of MTR and material transfer (MT) with time at Ip 8 A, and T_{on} 256 µs, with

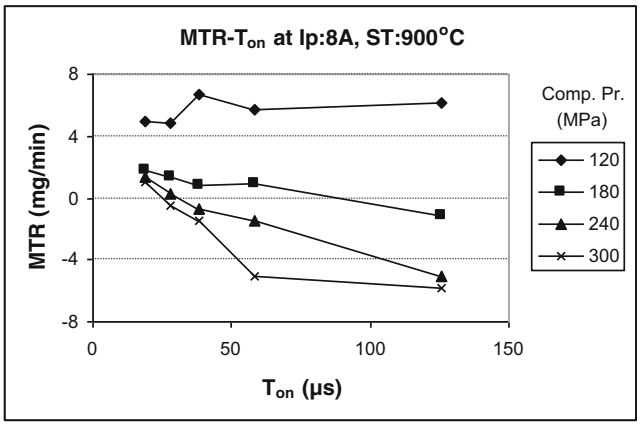

(a)

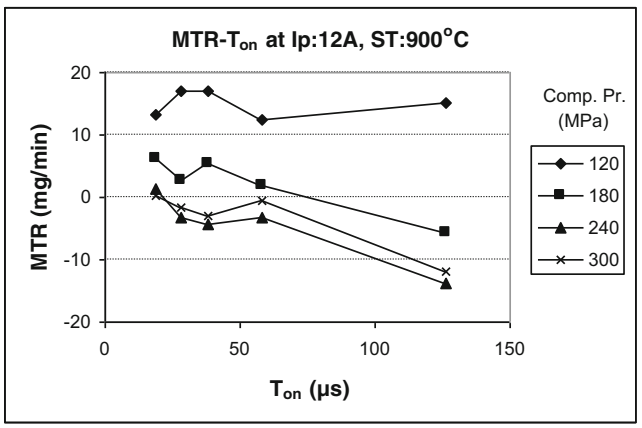

(b)

Fig. 5 The variation of MTR with T_{on} at different compaction pressures, at ST 900 °C and **a** Ip 8 A, **b** Ip 12 A

tools of 120 MPa and 700 °C are shown in Fig. 7a, b, respectively. Here, MTR declines with time and the trend is shown in the plot. The MT increases with time and its trend is also shown in the same figure.

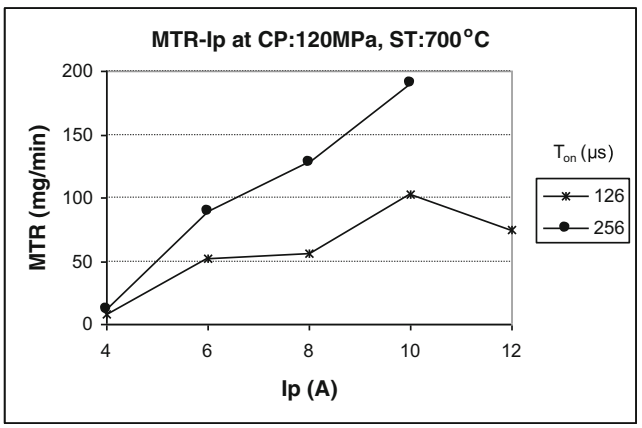

Fig. 6 The variation of MTR with Ip for two T_{on} settings at CP 120 MPa, and ST 700 °C

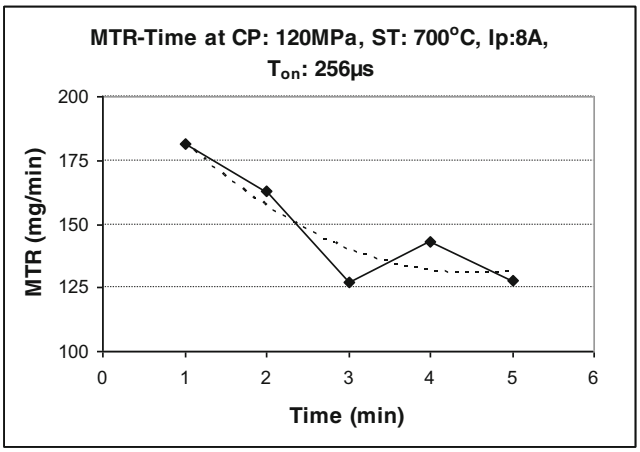

(a)

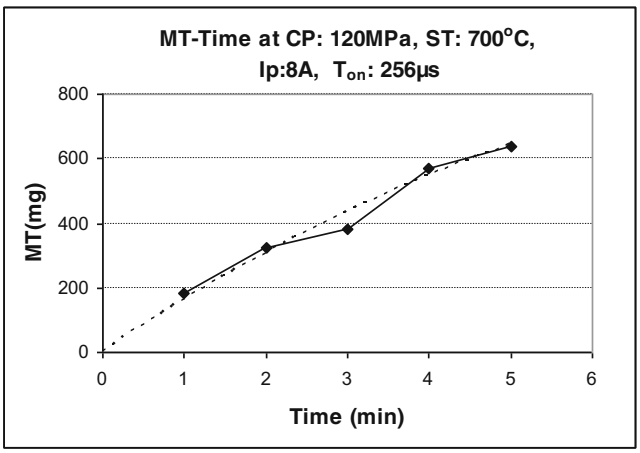

(b)

Fig. 7 **a** MTR and **b** MT with the variation of time

3.3 Tool wear rate

Tool wear rate (TWR) was also studied during the experimentation. It was measured in the same way as the MTR. The effect of various parameters on tool wear rate can be seen in Figs. 8, 9, 10, and 11, and from these plots, the following points can be drawn.

- The variation of TWR with T_{on} at different compaction pressure for Ip 4, 8, and 12 A and sintering temperature 700 and 900 °C is shown in the plots of Figs. 8 and 9. Here, it can be seen that with the increase in T_{on}, the TWR increases. In the same plots, it can also be observed that TWR is higher at lower compaction pressure than that at higher compaction pressure and this effect is more prominent at higher T_{on} settings. The effect of sintering temperature can also be witnessed in these plots. The TWR is higher at lower sintering temperature, i.e., 700 °C than that at higher sintering temperature, i.e., 900 °C. This is because, the tools sintered at 700 °C are much loose in their bonding and thereby wears more than the tools sintered at 900 °C.

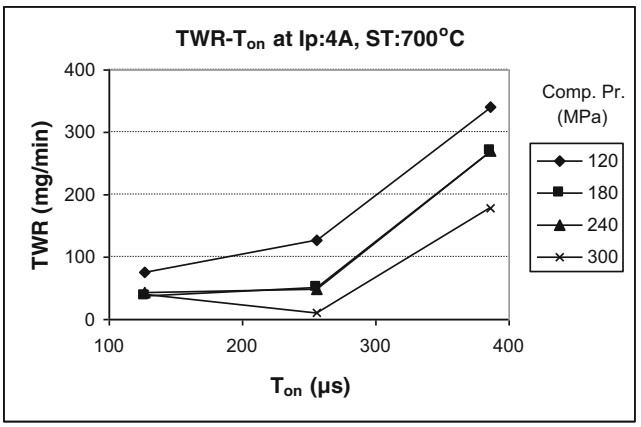

(a)

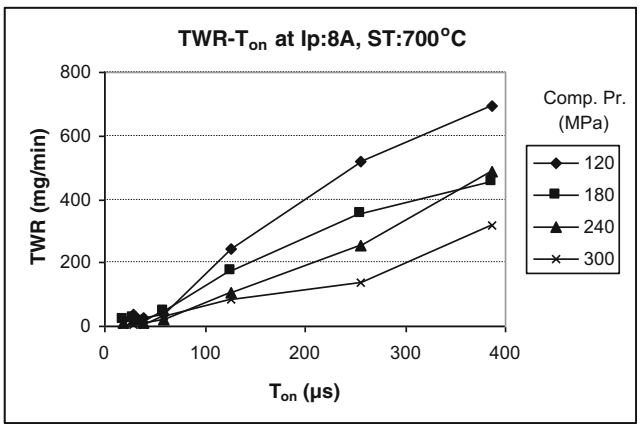

(b)

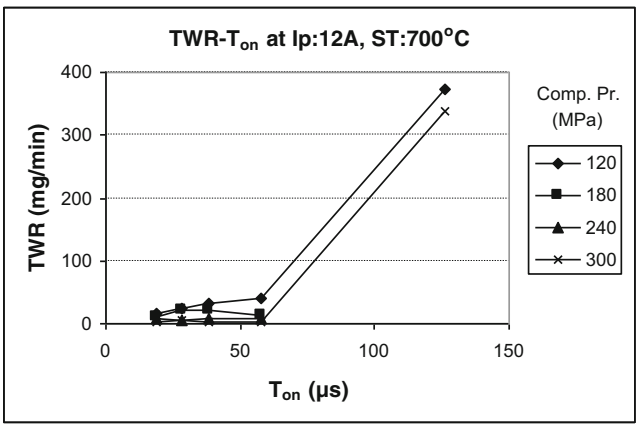

(c)

Fig. 8 The variation of TWR with T_{on} at different compaction pressures, at ST 700 °C and **a** Ip 4 A, **b** Ip 8 A, **c** Ip 12 A

- Figure 10 shows variation of TWR with Ip setting for two T_{on} settings of 126 and 256 µs at compaction pressure of 120 MPa. Here, it is very clear that with the increase in Ip setting TWR increases. At higher T_{on} settings, it is more than that at lower T_{on} settings.
- The trend of TWR and tool wear (TW) with the variation of time is shown in Fig. 11. The tool wear increases with time but with decreasing wear rate.

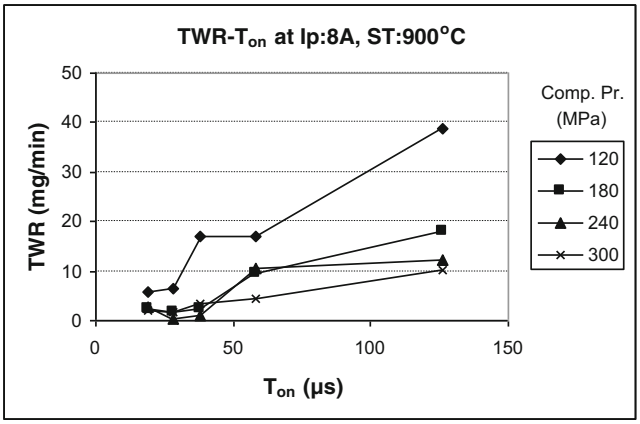

(a)

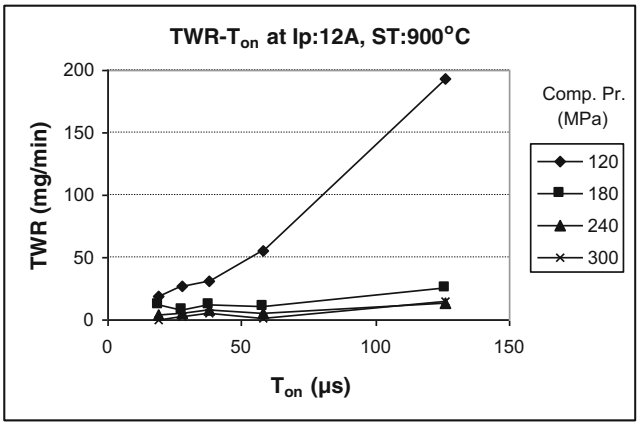

(b)

Fig. 9 The variation of TWR with T_{on} at different compaction pressures, at ST 900 °C, and **a** Ip 8A, **b** Ip 12A

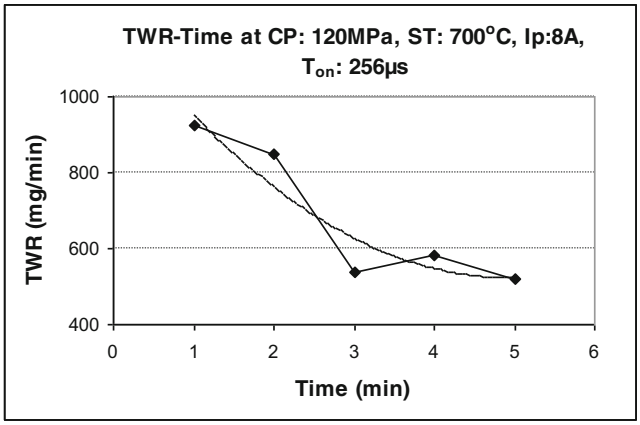

(a)

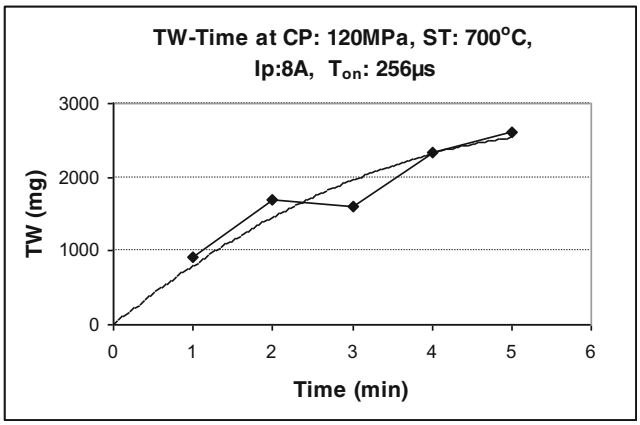

(b)

Fig. 11 Variation of **a** TWR and **b** TW with time

3.4 Surface topography

For surface roughness measurement, multiple readings were taken for each workpiece and average was considered. The variation of surface roughness in terms of R_a values with different parameters is shown in Figs. 12 and 13.

From these plots, the following points can be observed.

- In the plot of R_a–T_{on} at sintering temperature 700 °C, shown in Fig. 12, it can be observed that at Ip 4A (Fig. 12a), the surface is rougher at lower T_{on} whereas at higher T_{on} it is smoother. It is seen that in lower T_{on}, the deposition is not uniform, but at higher T_{on}, the deposition is much consistent giving rise to a uniform surface. In the plot of R_a–T_{on} at Ip: 8A (Fig. 12b), it is very evident that with the increase in T_{on} surface roughness increases. A good number of experiments were conducted at 8 A from T_{on} 19 to 386 µs. In the specimens processed with 8 A current setting, it is seen that the deposition is uniform throughout. At Ip setting of 12 A (Fig. 12c), the experiments were conducted at lower T_{on} settings only. No clear trend is seen in these experiments.
- In the plots of R_a–T_{on} at sintering temperature 900 °C, shown in Fig. 13a, b, an increasing trend of R_a with T_{on} is seen in both 8- and 12-A settings. Particularly at

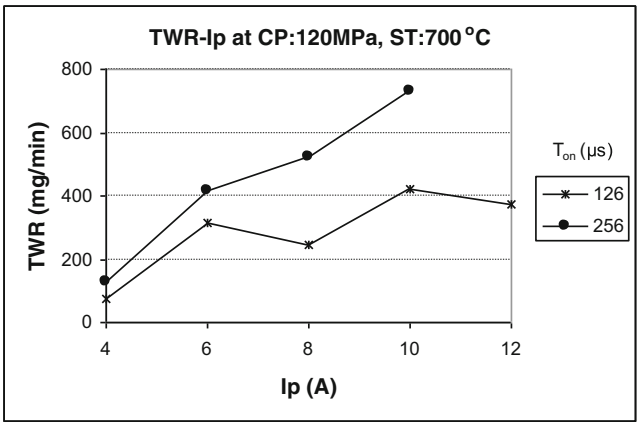

Fig. 10 Variation of TWR with Ip for two T_{on} settings at CP 120 MPa, and ST 700 °C

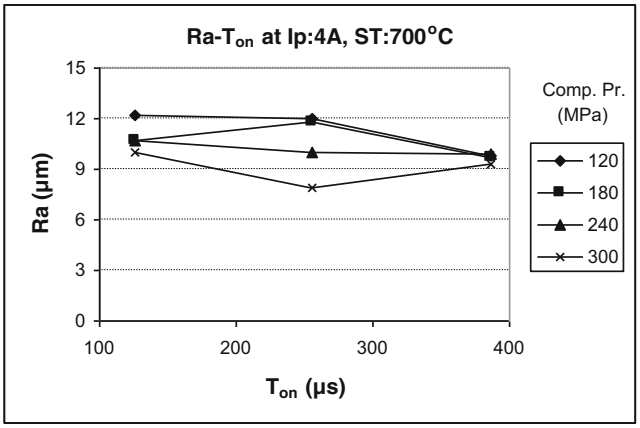

(a)

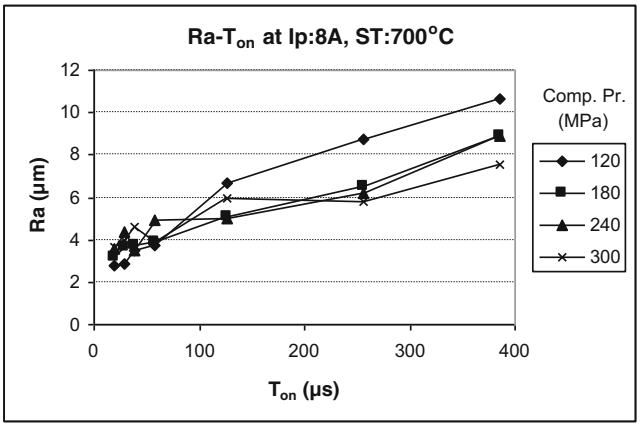

(b)

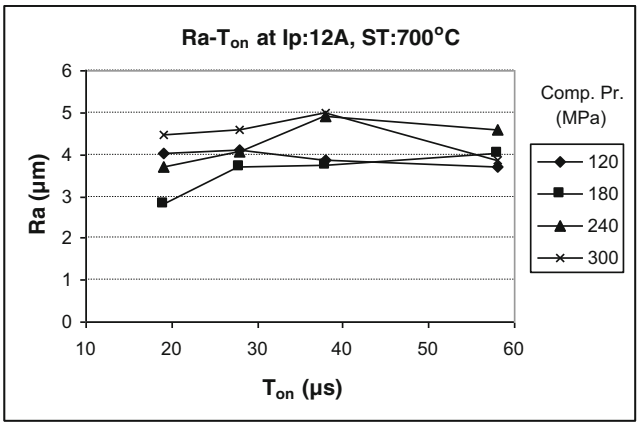

(c)

Fig. 12 The variation of R_a with T_{on} at different compaction pressures at ST 700 °C and **a** Ip 4 A, **b** Ip 8 A, **c** Ip 12 A

compaction pressure 120 MPa, the surface roughness is more than the others cases.

- In the same plots shown in Figs. 12 and 13, for both the sintering temperatures, a decreasing trend of R_a value with increase in compaction pressure is seen especially at higher T_{on} settings. At lower T_{on} settings, the variation of R_a is in a band of 3–6 µm in general.

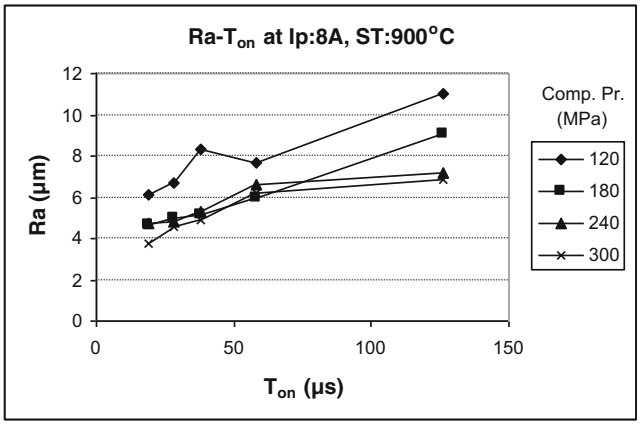

(a)

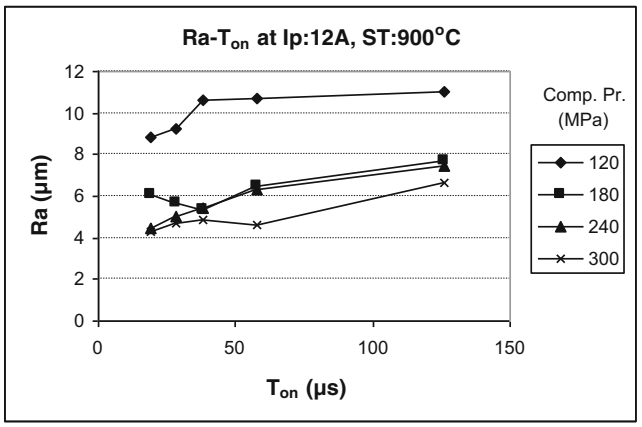

(b)

Fig. 13 The variation of R_a with T_{on} at different compaction pressure at ST 900 °C, and **a** Ip 8 A, **b** Ip 12 A

3.5 Deposited layer

The representative images of transverse section of workpieces, having a good amount of deposited material at the top, are shown in Fig. 14. The optical micrographs of transverse section of some work specimens, having a very thin to a

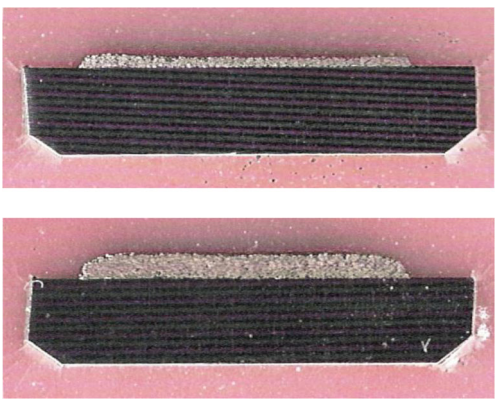

Fig. 14 Images of transverse section of workpieces with thick deposited layer

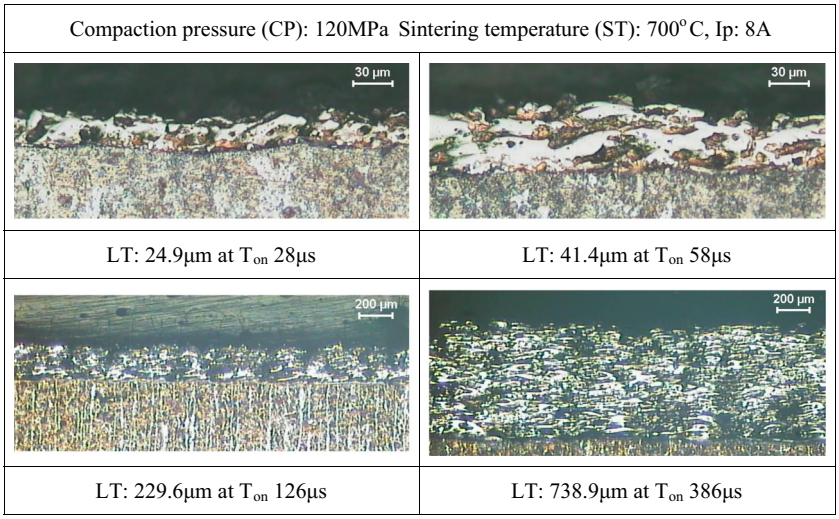

Fig. 15 Optical micrographs of transverse section of some samples showing deposited layer and its thickness (LT) at CP 120 MPa, ST 700 °C, Ip 8 A and at different T_{on}

moderately thick layer obtained under varying conditions, are shown in Fig. 15. It can be seen that at compaction pressure of 120 MPa, sintering temperature of 700 °C, and Ip of 8A, the layer thickness increases with the increase of T_{on}. A wide range of the deposited layer can be witnessed from these micrographs. Magnified image of the transverse section of the deposited layers showing different zones and corresponding values of microhardness is shown in Fig. 16. Irrespective of the layer thickness, it is observed that the deposited layer is composed of different materials making a composite structure. It has unetched bright and hard zones of tungsten and its carbides. At some pockets, there is evidence of copper which acts as binder. The white zones seen in the micrographs are very hard as compared to other zones and are having microhardness in the order of 9.8 to15.7 GPa. It has also been observed that the hardness increases just below the layer as compared to that of the base metal because of possible structural changes in solid state. The microhardness, in a particular section is taken from lower portion of the layer to the base metal along depth. The variation of the microhardness along depth is shown in Fig. 17. At the white zone of the layer, the microhardness is quite higher (15.5 GPa), at the lower portion of the white zone in the layer, it is moderately high (9.0–9.8 GPa), and at the base just below the layer it is more than the base metal (3.5 GPa), and it gradually decreases to the hardness of base metal (2.1–2.3 GPa).

The effect of various parameters on average layer thickness (LT) can be observed in the plots shown in Figs. 18, 19, 20, and 21. From these plots following points can be observed:

- From the plots of LT-T_{on} at various compaction pressures for tools with ST: 700 °C and Ip: 4A and 8A as shown in Fig. 18a, b, it is evident that the average layer thickness (LT) increases with T_{on}. This trend is very much clear at higher T_{on} settings. At lower T_{on}, LT is comparatively very thin and their variation is not very prominent. At Ip 12 A also (Fig. 18c), not a very distinctive trend is seen at the lower T_{on} settings. From these set of plots, it can also be observed that with the increase of compaction pressure, the average layer thickness decreases. But this trend is prominent in higher T_{on} settings only. This trend is not that clear at Ip 12 A as the experiments were conducted in lower T_{on} settings only (Fig. 18c). Moreover at 12 A, discharge phenomenon is not stable because of the poor withstanding capacity of loosely bonded tools at higher current load.
- From the plots for tools with ST 900 °C and Ip 8 and 12 A, as shown in Fig. 19a, b, the trend of LT with T_{on} is not

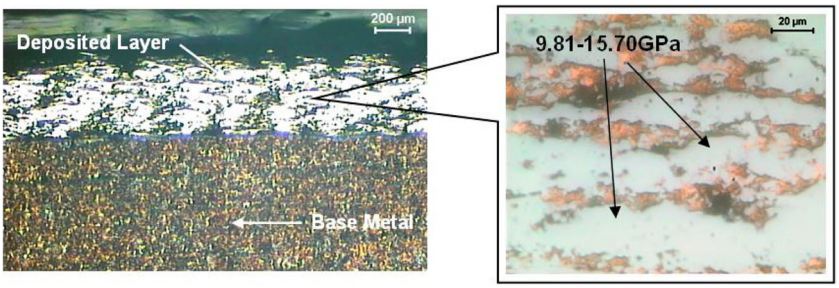

Fig. 16 Transverse section of a workpiece sample with very thick layer and a magnified image of the same layer, showing microhardness at hardest zones

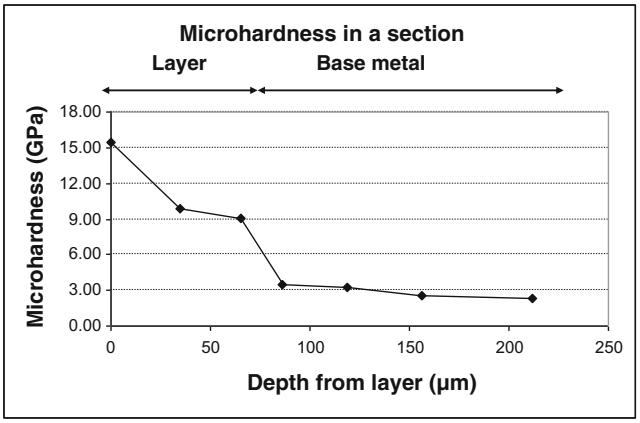

Fig. 17 Variation of microhardness from a portion of a layer to base metal

clear. With the tools of compaction pressure 120 MPa, the layer thickness is comparatively more than that at other higher compaction pressures. It can be seen that with the increase of compaction pressure the LT decreases. In this category of experiments, it is seen that there is no net addition of material in all the cases. So, the achieved layer is not always due to just addition of material but also due to recast or redeposition of material having some interaction with tool material.

- The variation of LT with Ip, at compaction pressure 120 MPa, sintering temperature 700 °C and T_{on} settings 126 and 256 μs is shown in Fig. 20. It is quite evident here that with the increase in Ip, LT increases at these higher T_{on} settings. Moreover, it can also be observed that at 256 μs, the LT is more than that at 126 μs.
- At compaction pressure of 120 MPa, sintering temperature of 700 °C, Ip of 8A, and T_{on} of 256 μs, LT shows an increasing trend with time, as shown in Fig. 21.

3.6 SEM analysis

The scanning electron micrographs (SEM) of top surface of workpieces after EDM exhibiting three typical cases are shown in Fig. 22. A very fine and thin deposited surface, a very thick deposited surface, and a surface due to material removal rather than addition of tool material are shown in Fig. 22a, b, c respectively. The process parameters like compaction pressure (CP), sintering temperature (ST), peak current setting (Ip), and on time (T_{on}) are also mentioned in the respective figures. From these figures, it is evident that for Ip settings (here 8 and 10 A) for which there is free flow of material with regular sparking, the deposited surface is very thin and fine at low T_{on} settings and the same is thick and relatively coarse at high T_{on} settings. The high T_{on} provides more energy and helps in having more material transfer by melting and dislodging more material from the tool and

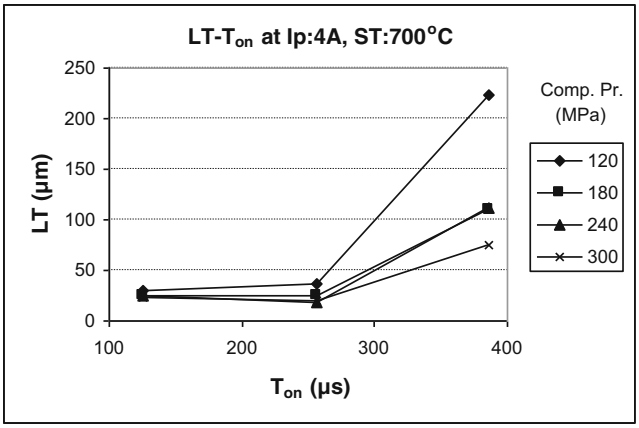

(a)

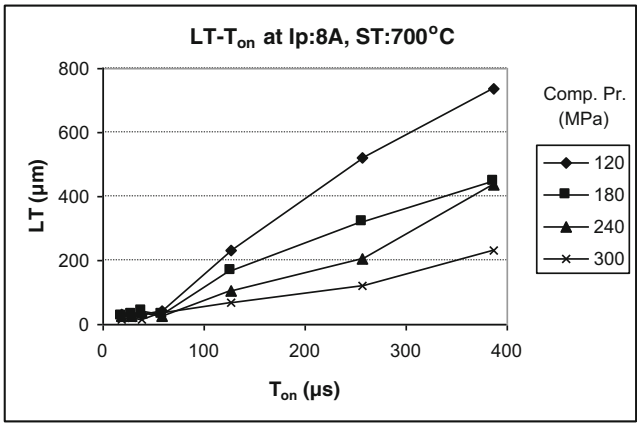

(b)

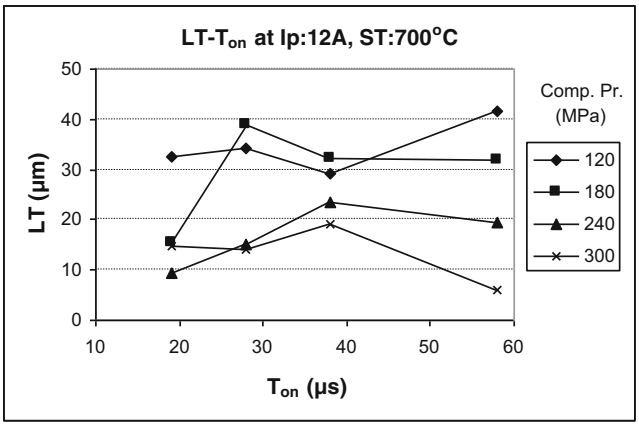

(c)

Fig. 18 The variation of LT with T_{on} at different compaction pressures, at ST 700 °C, and **a** Ip 4 A, **b** Ip 8 A, **c** Ip 12 A

getting it deposited on the work surface. The tools compacted at higher compaction pressure and sintered at higher temperatures do not allow mass transfer from tool but results in material removal. For samples processed with tools compacted at 300 MPa, sintered at 900 °C and with Ip at 8 and 12 A there is no indication of deposition of tool material over the surface. The microstructure of these samples is very much different from the other samples. In such cases, the

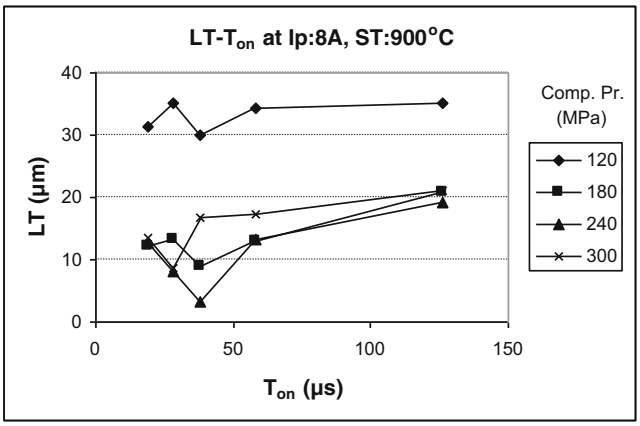

(a)

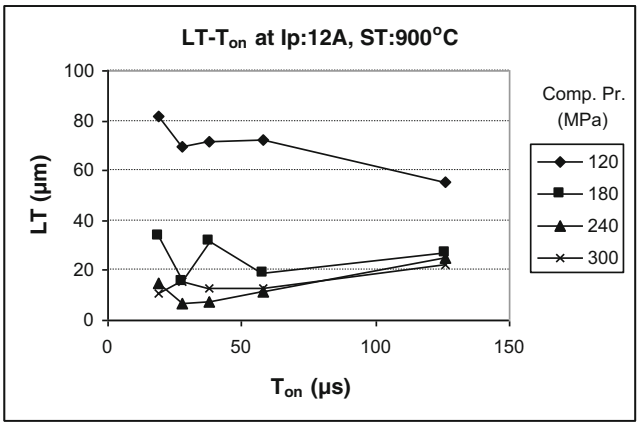

(b)

Fig. 19 The variation of LT with T_{on} at different compaction pressures, at ST 900 °C, and **a** Ip 8 A, **b** Ip 12 A

resulted surface is by redeposition or recast of molten material with some interaction with tool material.

3.7 EDX analysis

EDX analysis was performed on the top surface of the EDMed samples to confirm the transfer of tool material over the

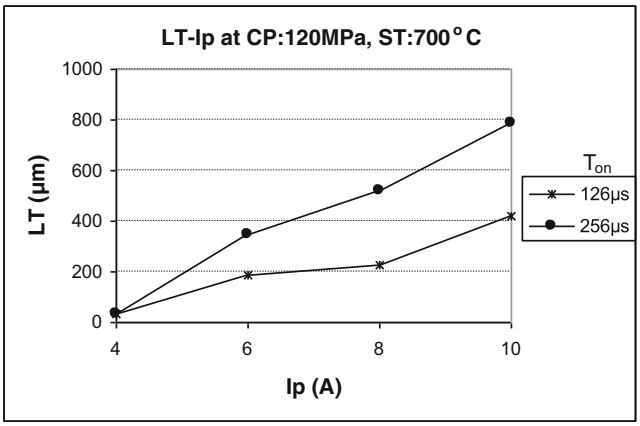

Fig. 20 The variation of LT with Ip for two T_{on} settings at CP 120 MPa, and ST 700 °C

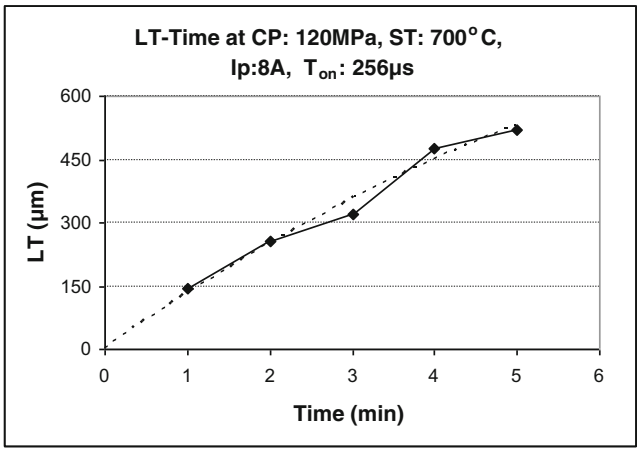

Fig. 21 LT with the variation of time

workpiece surface and also to assess the quantitative value of each element in the deposited layer. The EDX was performed at two conditions of the samples, one is "as it is" condition after EDM and other is after removing a few microns from the top deposited surface and then polishing. The quantitative results of elemental analysis for different experimental conditions are depicted in the form of bar charts.

At first, bulk analysis was done on the EDMed surface in "as it is" condition without any post processing and element percentages of Fe, Cu, and W were recorded. Figure 23 shows the EDX results of some samples with thin layer deposition at Ip setting of 8A and 12A and at other similar experimental conditions. The element percentages are almost same in all these cases. The percentage of W is higher than other elements. The percentage of Fe, which comes from base material, is low because the deposited layer is reasonably thick.

In second attempt, the top deposited surface was removed by a few microns and the samples were polished. The SEM and optical micrographs of the top surface of one of these polished samples processed at CP 120 MPa, ST 700 °C, Ip 8A, T_{on}: 386 µs are shown in Fig. 24. In this case, the deposition is thick and very much uniform. The white portion is the harder zone. A few pockets of copper can be identified in these micrographs. A few micro holes and gaps are also visible. The EDX is done first at bulk area in "as it is" condition and then on the bulk area on polished samples and the percent of the each element (Fe, Cu, and W) were recorded. EDX results of some samples with thick deposition at different T_{on} settings and at Ip 8A in "as it is" condition and 'polished' condition are shown in Fig. 25. The percent of W after polishing is higher than that in "as it is" condition.

In case of polished samples, percent of W is higher and percent of Cu is lower than that in 'as it is' condition. From this observation, an important supposition can be made that Cu gets deposited at the top most part of the layer whereas W gets deposited in the inner part of the layer. This is much desirable to achieve a hard deposited layer. The white spots

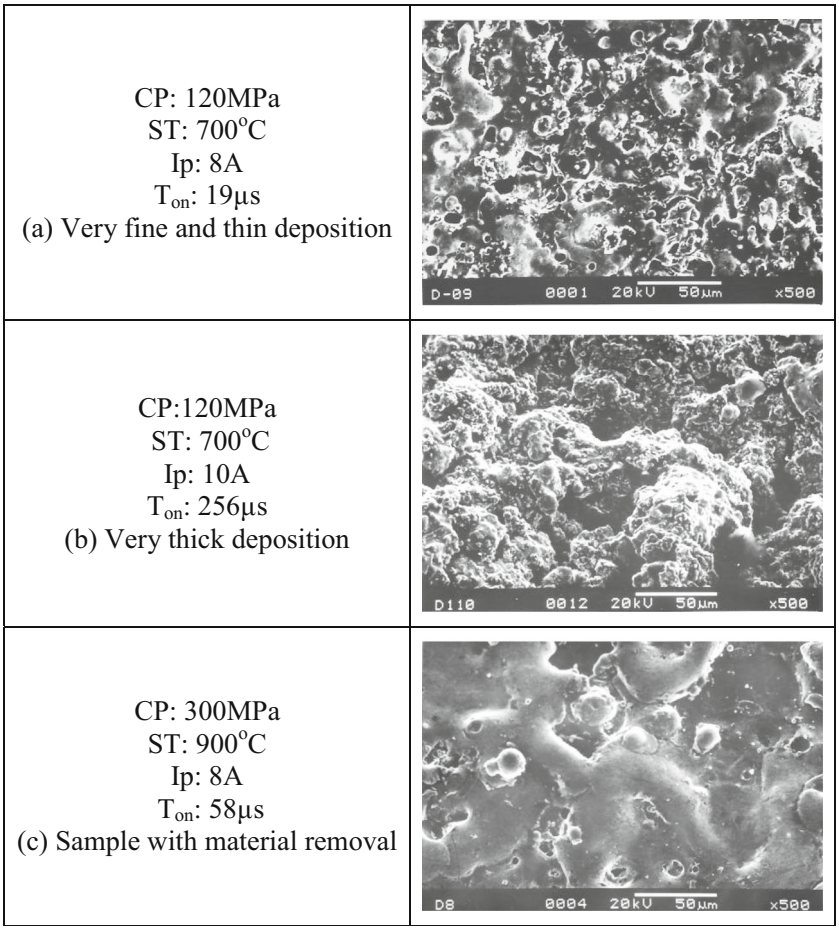

Fig. 22 SEM of the top surface of samples after EDM in various conditions

shown in the optical micrographs are much harder than the other portion of the surface and this is due to the presence of sufficient amount of W and may be due to the possible formation of tungsten carbide. This establishes a very important fact that in the superficial layer the percent of Cu is high but the layer in the underneath is rich in W. This is very much enviable since W and its carbides are the main source to increase the hardness of the layer. The EDX plots showing different peaks representing Fe, Cu, W, and C elements of one of the sample with thick layer in both 'as it is' condition and polished

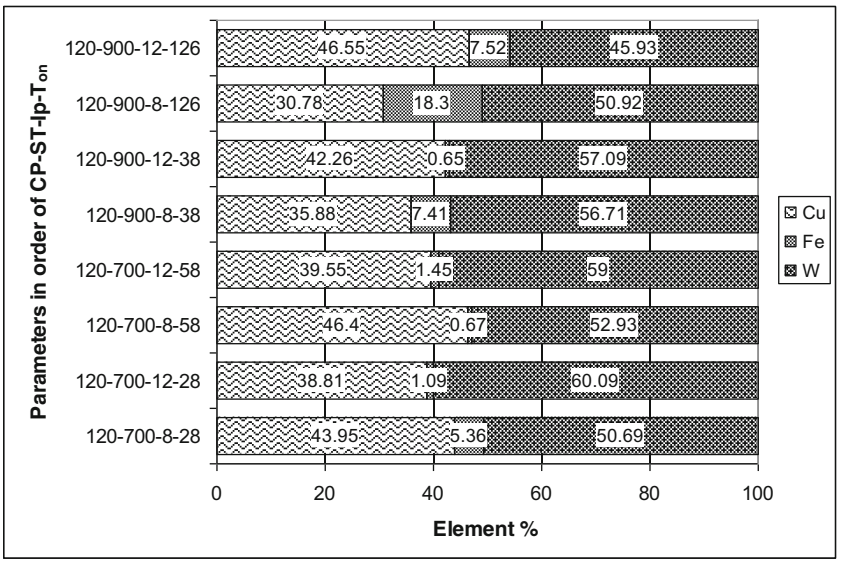

Fig. 23 EDX results of samples with thin deposition at 8 and 12 A at similar conditions

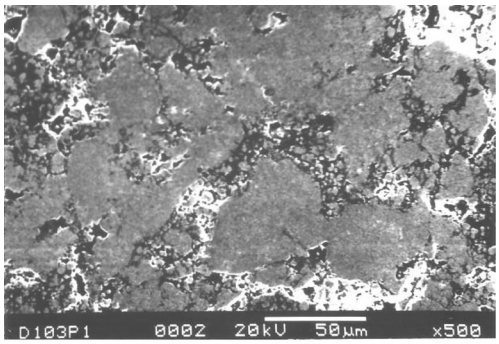

SEM

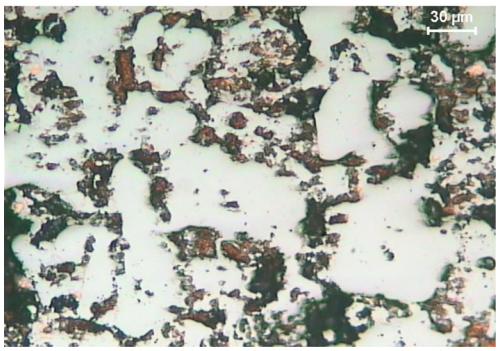

Optical

CP: 120MPa, ST: 700° C, Ip: 8A, T_{on}: 386µs

Fig. 24 Micrographs of one of the polished samples with thick deposition

condition, are shown in Fig. 26. This further ascertains the same observations. In some of the experimental conditions, net material removal was observed rather than net material addition. In those samples, a very thin layer deposition was observed. EDX is done on the top surface of these samples and the EDX plot of one of these samples is shown in Fig. 27. The peaks of the elements Fe, Cu, and W are present in this plot. But one important observation is that even in case of material removal from the sample, W is present on the surface. This as well contributes towards the surface integrity of the sample and increases the hardness of the work surface. The intensity of the peak of Fe is very high compared to other elements and this indicates that the top surface is not thickly coated as in other cases.

3.8 EDX by line scan

EDX by line scan was done on some of the samples in transverse section from top of the deposited layer to some portion of substrate. This was done to observe the relative variation of elements C, Fe, Cu, and W along this direction. The details of the samples chosen for this analysis are given in Table 2. These samples are so chosen that layer by deposition and a layer by recast of material are included. The SEM images of transverse section of these samples are shown in Fig. 28. The EDX line-scan plots showing the relative variations of different elements along depth are shown in Fig. 29.

From these EDX line-scan plots the relative variation of elements like C, Fe, Cu, and W from surface to base metal can be observed. In case of sample 1 with a thin deposited layer, the EDX line-scan plot is shown in Fig. 29a. Here, it can be seen that the amount of C is comparatively very less and almost same throughout. The amount of Fe is less in the deposited portion and then increases along the base. In the deposited layer portion, it can be seen that the amount of W and Cu are maximum and decreases at the substrate. This means that the deposited layer is rich in W, Cu, and C only. Non-appreciable presence of Fe at the layer indicates there is no formation of any kind of compound/alloy of Fe at the deposited layer. In case of sample 4, there is no net addition of material but there is a thin layer due to the recast of materials. The EDX line-scan plot of this sample is shown in Fig. 29b. In

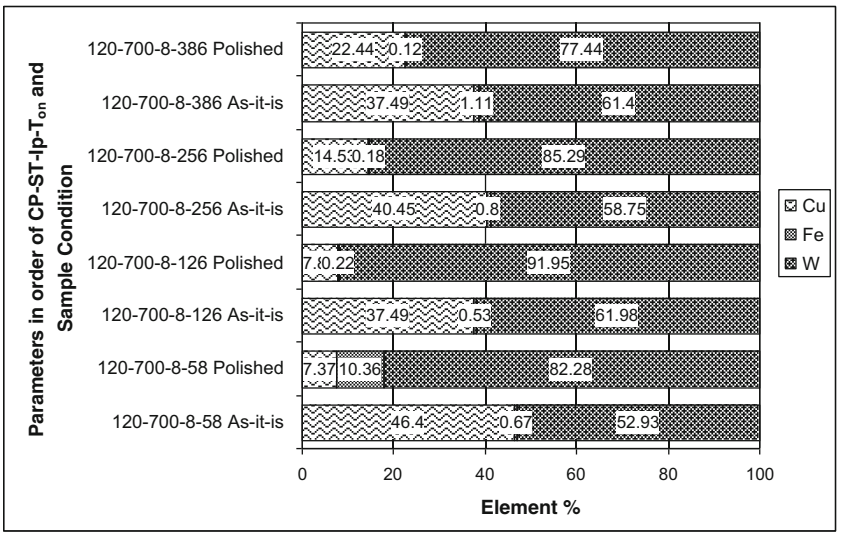

Fig. 25 EDX results of samples at different T_{on} settings at Ip 8 A in "as it is" condition and after polished

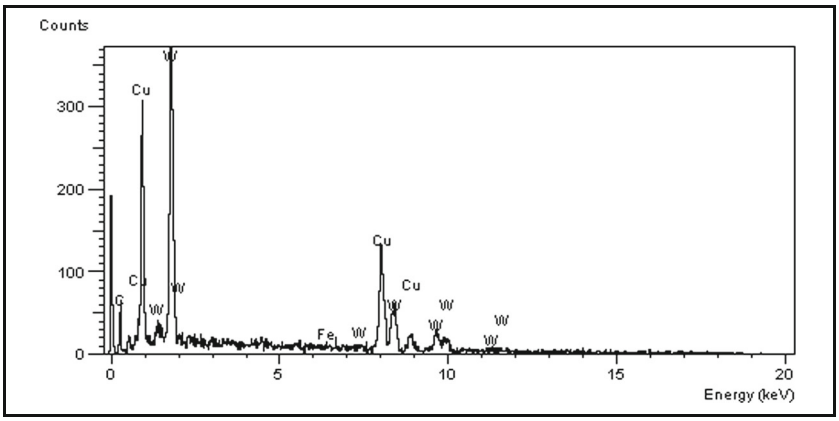

(a) As it is

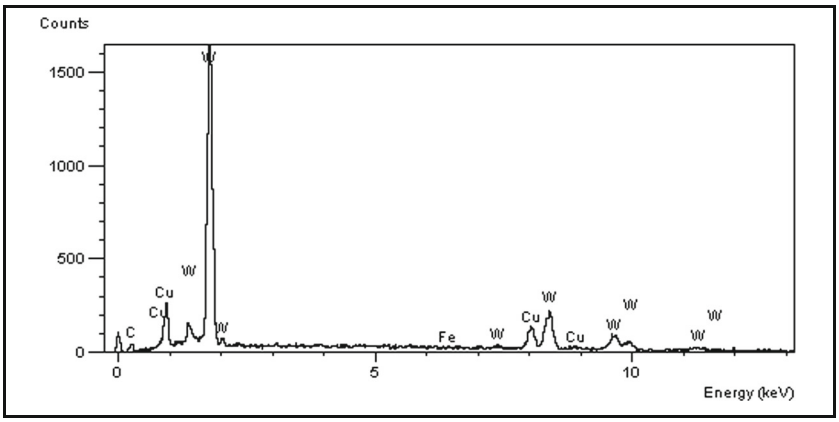

(b) Polished

Fig. 26 EDX plots showing peaks of different elements in **a** "as it is" and **b** "polished"

Sample parameters: CP: 120MPa, ST: 700°C, Ip: 8A, T_{on}: 256μs

this case, it can be seen that at the layer C is maximum and then decreases, Fe gradually increases from surface to the base metal and reaches to maximum. A very small amount of W and Cu is present at the layer and just below the layer at the substrate and gradually decreases towards base metal. From this it can be inferred that in the recast layer the chances of formation of carbides of Fe and W are there. Some trace amount of W and Cu might have diffused in the substrate.

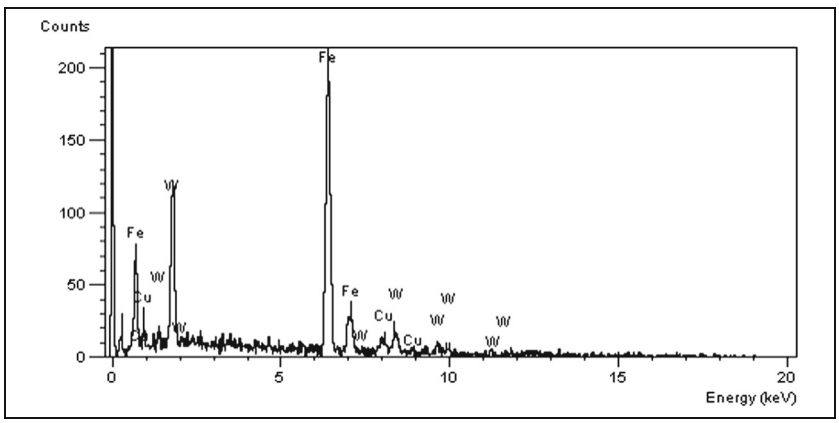

Sample parameters: CP: 300MPa, ST: 900°C, Ip: 12A, T_{on}: 38μs

Fig. 27 EDX plot of a sample with material removal

Table 2 Details of samples studied for EDX line scan

Sample no.	Parametric conditions				LT (μm)	Remarks
	CP (MPa)	ST (°C)	Ip (A)	T_{on} (μs)		
1	120	700	8	58	41.4	Thin layer by deposition
2	300	900	8	126	21.0	Very thin layer by recast of material

3.9 XRD analysis

X-ray diffraction (XRD) analysis was carried out to confirm the transfer of tool material on the work surface and also to identify the phases of any compound formed during the EDM process. The top deposited layers of some of the samples were analyzed. The XRD plot of a typical case is shown in Fig. 30. The peaks of W, W_2C, Cu, and Fe can be seen in this plot. This confirms that the tool materials W and Cu get transferred to the work surface. Tungsten carbide (W_2C) is formed on the deposited layer and that creates the hard phase in the layer.

4 Discussions

A detailed study has been performed on surface modification phenomena by W–Cu P/M sintered compact tools. The process has been successfully implemented for surface modification of C-40 grade steel. A wide variation in results has been achieved for the entire range of study. The results are subsequently discussed.

In the study of surface modification with W–Cu P/M tools, the following four major types of phenomena are observed.

1. *Material removal process rather than material addition.* This is seen where the tools are having good compaction

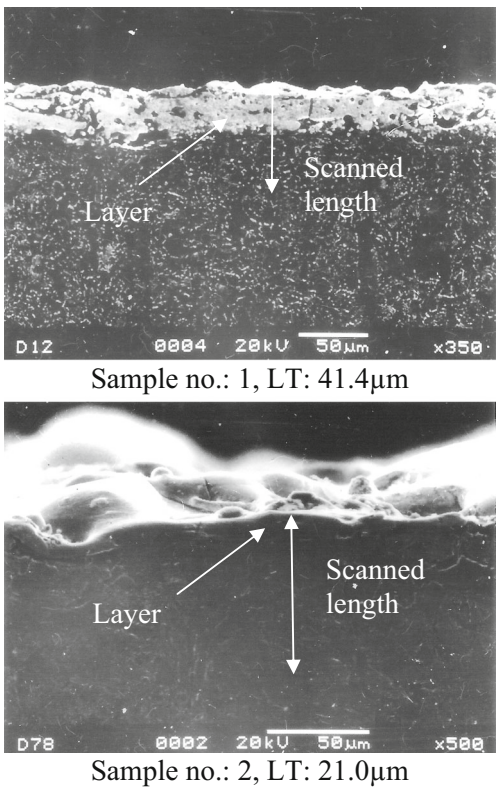

Fig. 28 SEM images of transverse section of samples studied for EDX line scan

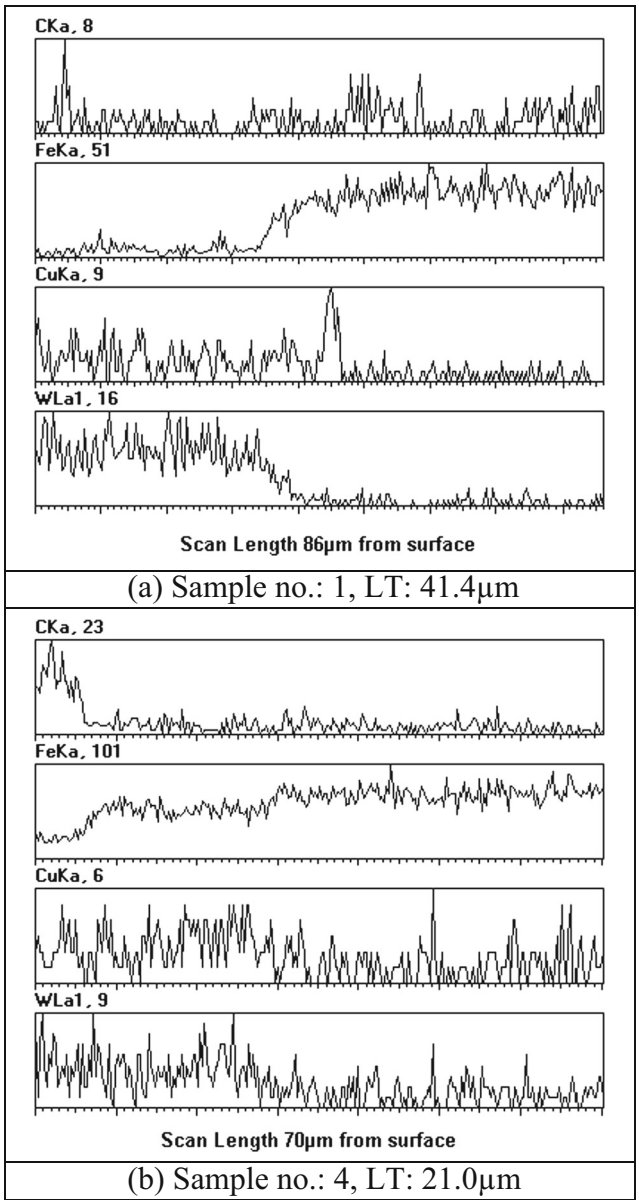

Fig. 29 EDX line-scan plots showing the element variations

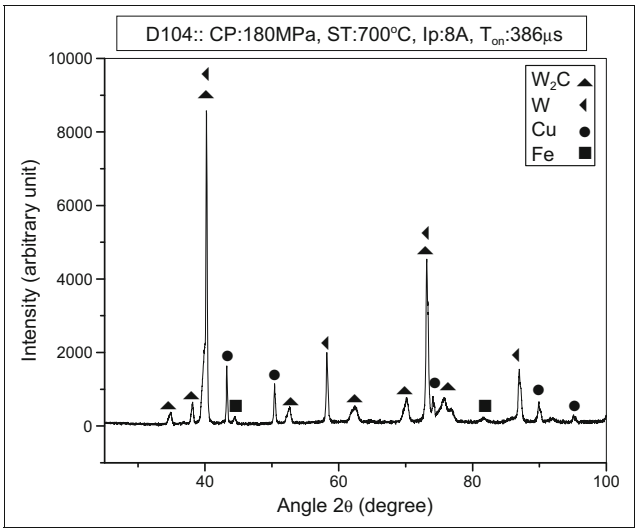

Fig. 30 XRD Plot of a sample processed at Ip 8 A and T_{on} 386 μs with tool compacted at 180 MPa and sintered at 700 °C (Cu target)

and well-sintered, mostly in case of the tools compacted at higher pressures and sintered at 900 °C. In these tools, the material particles are bonded well, so this is not a favorable condition for material transfer. Here, a thin hard layer is seen over the work surface, which is basically a white layer consisting of work material, a little of tool material and the dissociated carbon particles from dielectric fluid.

2. *A thin uniform layer over the work surface with material addition.* This phenomenon is seen where the particles of tool material are loosely bound and the EDM parameters are selected in the lower range. Due to the supply of less intense energy during the process, the tool wear rate is slow, which results in a thin deposited layer over the work surface.
3. *A highly damaged irregular surface with material addition,* This type of condition is seen when the tool particles are loosely bound as in case of tools sintered at 700 °C and the EDM parameters are in the higher side, as seen in case of Ip 12 A at higher T_{on} settings. Here, the tools cannot withstand such an intense energy and results in lump detachment of tool materials and irregular deposition over the work surface. These lumps are also the major cause of bridging the gap between the tool and the workpiece resulting in formation of arcing and short circuiting, which further deteriorates the work surface. This phenomenon is very much undesirable.
4. *Relatively thick and uniformly deposited layer with material addition.* This is the condition where a good amount of material gets deposited uniformly over work surface, as in the cases with the tools sintered at 700 °C and processed at Ip 8 A. The major constituent of the deposited layer is the tool materials and their compounds. This is the outcome of an optimum parametric combination and is the most desirable. Here, the tool wear is very high but in a uniform manner. There is neither any indication of lump deposition nor any formation of big crater over the work surface.

5 Conclusions

After conducting a number of studies on the deposited surface, the final conclusions can be drawn as follows:

1. Photographs of some representative samples showing the work surface after EDM operation can give the first visual impression of the outcome of the process.
2. A wide spectrum of MTR is achieved from nearly 1 to 191 mg/min in different conditions. Material removal is also seen in some case. The graphical representation of variation of MTR with different controlling parameters is presented and discussed.
3. In favorable conditions, very uniformly deposited surfaces are obtained. The R_a values of the work surface are obtained in the range of 3 to 15 μm. But in some extreme conditions, where there is a good deposition of material, the R_a values are in the range of 8 to 10 μm. The R_a values in different experimental conditions are presented in graphical forms.
4. The average layer thickness varies in a wide range from nearly 3 to 785 μm over the work surface. The variation of layer thickness (LT) with various parameters is presented. The optical micrographs of the transverse section of workpiece sample are presented which reveal the microstructures of the deposited layer.
5. As the deposited layer is of composite structure, the hardness is not same throughout. In the harder zone the microhardness is obtained in the range of 9.8 to 15.7 GPa. Just below the deposited layer, the increase in hardness is observed. A gradual increase in hardness from base to the deposited layer is also observed.
6. SEM micrographs of the top surface of EDMed samples indicate how the material is deposited over the work surface and how the deposited layer is different than the machined surface by EDM.
7. EDX analysis is presented which confirms the transfer of tool materials over the work surface. The plots showing the peaks of different elements (W, Cu, Fe, and C) are presented. Quantitative evaluation of transferred material is carried out and presented in the form of bar charts. It is observed that whenever there is a good amount of material transfer, the major element is W, which is around 45 to 60 %; Cu is in the range of 35 to 45 % and rest comprises of very little amount of Fe. EDX is also done on the EDMed surface after removal of a few microns from the

top layer. In this case, it is observed that W is present around 80 % or more, and Cu is in the range of 7 to 22 %.

8. EDX analysis with line scan has also been done from deposited layer to the base metal. The plots depicting the variation of different elements along depth are presented. These confirm that the deposited layer is reach in W and Cu.
9. XRD analysis confirms the presence of tool material over the work surface and formation of carbide in the deposited layer. It is seen that W is transferred to the work surface in elemental form as well as in the form of carbides like W_2C mostly.

This study establishes the use of W–Cu P/M sintered compact tools for surface modification of C-40 grade steel by transferring the tool material in elemental form as well as in the form of compounds. These deposited materials form a hard and composite layer over the work surface. The detailed characterization of the deposited layer is presented, which will be the manifestation for further research in this area.

References

1. Rajurkar KP, Pandit SM (1984) Quantitative expressions for some aspects of surface integrity of electro discharge machined components. Trans ASME J Eng Ind 106:171–177
2. Lim LC, Lee LC, Wong YS, Lu HH (1991) Solidification microstructure of electrodischarge machined surfaces of tool steels. Mater Sci Technol 7:239–248
3. Rebelo JC, Dias AM, Kremer D, Lebrun JL (1998) Influence of EDM pulse energy on the surface integrity of martensite steels. J Mater Process Technol 84:90–96
4. Cusanelli G, Wyser AH, Bobard F, Demellayer R, Perez R, Flükiger R (2004) Microstructure at submicron scale of the white layer produced by EDM technique. J Mater Process Technol 149:289–295
5. Gangadhar A, Shunmugam MS, Philip PK (1991) Surface modification in electrodischarge processing with a powder compact tool electrode. Wear 143(1):45–55
6. Shunmugam MS, Philip PK, Gangadhar A (1994) Improvement of wear resistance by EDM with tungsten carbide P/M electrode. Wear 171:1–5
7. Samuel MP, Philip PK (1997) Power metallurgy tool electrodes for electrical discharge machining. Int J Mach Tools Manuf 37:1625–1633
8. Mohri N, Saito N, Tsunekawa Y, Kinoshita N (1993) Metal surface modification by electrical discharge machining with composite electrode. Anal CIRP 42(1):219–222
9. Fukuzawa Y, Kojima Y, Sekiguchi E, Mohri N (1993) Surface modification of stainless steel by electrical discharge machining. ISIJ Int 33(9):996–1002
10. Fukuzawa Y, Kojima Y, Tani T, Sekiguti E, Mohri N (1995) Fabrication of surface modification layer on stainless steel by electrical discharge machining. Mater Manuf Process 10(2):195–203
11. Mohri N, Fukusima Y, Fukuzawa Y, Tani T, Saito N (2003) Layer generation process on work-piece in electrical discharge machining. Anal CIRP 52(1):157–160
12. Moro T, Mohri N, Otsubo H, Goto A, Saito N (2004) Study on the surface modification system with electrical discharge machine in the practical usage. J Mater Process Technol 149:65–70
13. Tsunekawa Y, Okumiya M, Mohri N (1994) Surface modification of aluminium by electrical discharge alloying. Mater Sci Eng A174: 193–198
14. Tsunekawa Y, Okumiya M, Mohri N, Kuribe E (1997) Formation of composite layer containing TiC precipitates by electrical discharge alloying. Mater Trans JIM 38(7):630–635
15. Pantelis DI, Vaxevanidis NM, Houndri AE, Dumas P, Jeandin M (1998) Investigation into application of electrodischarge machining as steel surface modification technique. Surf Eng 14(1): 55–61
16. Simao J, Aspinwall D, El-Menshawy F, Meadows K (2002) Surface alloying using PM composite electrode materials when electrical discharge texturing hardened AISI D2. J Mater Process Technol 127:211–216
17. Simao J, Lee HG, Aspinwall DK, Dewes RC, Aspinwall EM (2003) Workpiece surface modification using electrical discharge machining. Int J Mach Tools Manuf 43:121–128
18. Aspinwall DK, Dewes RC, Lee HG, Simao J, McKeown P (2003) Electrical discharge surface alloying of Ti and Fe workpiece materials using refractory powder compact electrodes and Cu wire. Anal CIRP 52(1):151–156
19. Lee HG, Simao J, Aspinwall DK, Dewes RC, Voice W (2004) Electrical discharge surface alloying. J Mater Process Technol 149:334–340
20. Wang ZL, Fang Y, Wu PN, Zhao WS, Cheng K (2002) Surface modification process by electrical discharge machining with a Ti powder green compact electrode. J Mater Process Technol 129: 139–142
21. Tsai HC, Yan BH, Huang FY (2003) EDM performance of Cr/Cu-based composite electrodes. Int J Mach Tools Manuf 43(3):245–252
22. Akiyoshi M, Goto A, Mohri N, Saito N (2003) Planarization of a layer made by using electrical discharge machining. JSME Int J Ser A 46(3):496–501
23. Yan BH, Tsai HC, Huang FY (2005) The effect in EDM of a dielectric of a urea solution in water on modifying the surface of titanium. Int J Mach Tools Manuf 45(2):194–200
24. Zinelis S (2007) Surface and elemental alterations of dental alloys induced by electro discharge machining (EDM). Dent Mater 23(5): 601–607
25. Chen YF, Chow HM, Lin YC, Lin CT (2008) Surface modification using semi-sintered electrodes on electrical discharge machining. Int J Adv Manuf Technol 36:490–500
26. Patowari PK, Mishra UK, Saha P, Mishra PK (2010) Surface modification of C40 steel using WC-Cu P/M green compact electrodes in EDM. Int J Manuf Technol Manag 21(1/2):83–98
27. Patowari PK, Saha P, Mishra PK (2011) Taguchi analysis of surface modification technique using W-Cu powder metallurgy sintered tools in EDM and characterization of the deposited layer. Int J Adv Manuf Technol 54:593–604
28. Patowari PK, Mishra UK, Saha P, Mishra PK (2011) Surface integrity of C-40 steel processed with WC-Cu powder metallurgy green compact tools in EDM. Mater Manuf Process 26:668–676